Title Page

USGS award number G11AP20050

Paul W. Jewell

LiDAR Signatures of Hydrothermal Alteration Features, Selected Mining Districts, Utah and Oregon

Research supported by the U.S. Geological Survey (USGS), Department of the Interior, under USGS award number G11AP20050. The views and conclusions contained in this document are those of the authors and should not be interpreted as necessarily representing the official policies, either expressed or implied, of the U.S. Government.

INTRODUCTION

The conterminous United States is now considered a mature province for the exploration and discovery of new ore deposits. It is fair to assume that most major ore deposits close to the surface or with clearly delineated surface alteration have been found. Continued discovery of new ore bodies in the U.S. and worldwide therefore depends on developing methods capable of imaging the subsurface or detecting alteration and mineralization patterns at the Earth's surface that are not apparent with traditional exploration techniques.

It has also been long been known that a number of geologic features have recognizable surficial spatial patterns that disrupt the physical nature of preexisting geologic units. These patterns are often difficult to detect during cursory field examination and are particularly problematic in areas of heavy vegetative or soil cover. While stratigraphic units and structural features such as faults have important surface manifestations, certain features of ore deposits do as well. For instance, the phyllic and advanced argillic alteration zones of porphyry copper deposits tend to weather recessively while the jasperoids and silicification associated with various types of precious metal deposits tend to be resistant to weathering and form prominent outcrops (e.g., *Lovering, 1972*; *Hedenquist et al., 2000*). Vein-type base metal deposits (which may be the expression of larger, concealed disseminated ore bodies) are often controlled by faults with a surface expression that is subtle or poorly expressed. As important as these features are, they often occur at scales that make them undetectable with traditional aerial photography where vegetation or poor resolution prevents their recognition.

In recent years, a promising new technology, "Light Detection and Ranging" – LiDAR – has been effectively applied to earth science as well as fields as diverse as art history and transportation engineering. Using a laser source, LiDAR is capable of producing remarkably fine-scale topographic maps and 3-dimensional images and can be used to detect subtle surface features on a wide variety of scales. The method relies on sending and receiving 10s of thousands of coherent laser pulses per second to the object being surveyed. One of the crowning achievements of airborne LiDAR has been its ability to "see through" vegetation and forest canopies based on "last return" of the laser pulses. In effect, post-processing of LiDAR data can filter out returns from tree and vegetative cover to reveal important features of the underlying land surface. As a result, unknown or poorly characterized fault scarps and landslides have been discovered and mapped (e.g., *Harding and Berghoff*, 2000; *Schulz, 2005*).

LiDAR instruments can be mounted on airborne or ground-based platforms. For airborne LiDAR, horizontal resolution can be as fine as 1-2 m while vertical resolution is on the order of a few centimeters. LiDAR has the potential to become a powerful 21st century tool for locating concealed ore deposits and may have the ability to be integrated with airborne geophysical methods and become effective in exploring in areas considered difficult for traditional exploration methodologies particularly terrain with extensive vegetation.

Using funding from the U. S. Geological Survey's Mineral Resources External Research Program, the author and several students at the University of Utah investigated the possibility of using LiDAR to indentify hydrothermal alteration features associated with a variety of historic mining districts. A large portion of the results are outlined below; a more succinct summary of the results will be published in the Society of Economic Geologists Newsletter (*Jewell et al.,* 2013).

METHODS

Data sets

The LiDAR data sets used in this project are publically available from the State of Utah and the Oregon LiDAR Consortium. Budgetary constraints prevented acquisition of new LiDAR strictly for the purposed of this project. The original MRERP proposal identified three mineral districts (Mt. Hood, North Santiam, and South Santiam/Blue River) in the Cascade Mountains of Oregon and two (Oquirrh Mountains and Alta) near the Wasatch Front of central Utah as having acceptable LiDAR coverage to conduct the project. It was subsequently discovered that northeastern Oregon and the Frisco mining district in southwestern Utah also contained both interesting mineralization features and the LiDAR coverage sufficient for investigation. Preliminary field investigations in the spring, 2011 showed Mt. Hood to not be an appropriate location for the study and difficulties in gaining access to private land in the Oquirrh Mountains disqualified this area from study. As a result, three localities in Oregon and two in Utah were subjected to detailed field investigations (Figure 1).

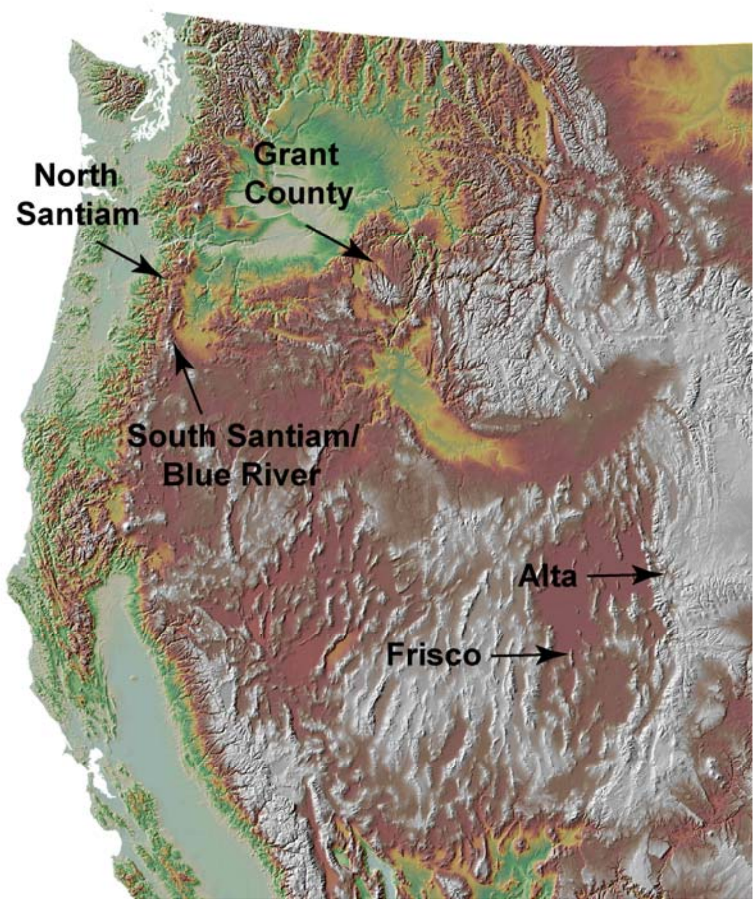

Figure 1. Location of mineral districts studied in this project.

The relevant, post-processed DEM files were downloaded from the internet or purchased for nominal cost and placed in ArcGIS during the first phases of the project. Following that, all available geologic maps and economic geology studies (including unpublished M.S. theses) of the areas covered by the LiDAR surveys were assembled. The maps from these studies were georeferenced and also downloaded into ArcGIS software.

Field work

Field work was performed between the summer, 2011 until the conclusion of the grant in June, 2012. The georeferenced data sets were field checked, described in detail, and the location recorded using hand-held GPS units. Where appropriate, geologic mapping at a scale of approximately 1:1000 was undertaken.

RESULTS

Alta District (Utah)

The Alta (also known as the Little Cottonwood-American Fork) and Park City mining districts in north-central Utah first became active in the 1860s and was productive until the period immediately following World War II. The district has largely produced from contact aureoles and fissures related to moderate-sized, intermediate to felsic intrusions that yielded mostly base metals and silver (*Boutwell*, 1912; *Calkins and Butler*, 1943). The Alta district is on the eastern edge of a 2006-2007 airborne LiDAR survey of the central Wasatch Front that was underwritten by the U.S. Geological Survey and a variety of local government entities.

Figure 2. Location of the mineralized areas examined within the Alta mining district.

Thaynes Canyon (contribution by Anna Farnsworth) Thaynes Canyon is located north of the main divide of the central Wasatch Range near the southwestern region of the Park City Mining District. The drainage is steep and heavily forested on the north-facing slopes. The little outcrop that exists is often cloaked by vegetation or glacial till. The geology of the canyon involves Triassic sedimentary formations that have been intruded by mid-Tertiary granodiorite stocks. The sedimentary units in the region are the Woodside Shale, a fine-grained dark-red shale, and the Thaynes Formation, a limey sandstone, and the Ankarah Formation composed of sandstone, mudstone, and shale (all of Triassic age). They strike northwest, with an average dip of 30° northeast. A series of northeast trending step faults have exaggerated the thickness of the Thaynes Formation (*Boutwell*, 1912). Deformation has also occurred near the gap at the head of the canyon where sedimentary rocks have been metamorphosed to marble and hornfels in a band 300-900 feet thick. West of Jupiter Hill the Thaynes Formation has recrystallized to skarn. The contact aureole is associated with the Clayton Peak Stock, a Mid-Tertiary quartz monzodiorite (*Bromfield*, 1989). The Clayton Peak Stock also contacts the younger Alta Stock west of Jupiter Hill. The Alta Stock is a granodiorite porphyry that has been intruded by a series of intermediate dikes that trend NE-SW. In places the porphyries exhibit propylitic alteration with epidote replacing feldspars and mafic minerals. The entire region has been glaciated and is largely covered by quaternary glacial deposits. On the canyon walls are several lateral moraines that appear to align with the intermediate dikes on the LIDAR image (Figure 3).

The canyon holds several mines including the Comstock, California, and Jupiter Mine. The only mine in range of the LIDAR data of this particular study is the Jupiter Mine. In its years of production (1882-1975), silver bearing lead ore was extracted from a mineralized fault zone. The fractures formed in a gap in the main divide which traverses the Thaynes Formation and a portion of the Woodside Shale and Ankarah Formation. The faults trend northeast and dip 45°-85°. The main shaft extends 800 feet and dips southeastward along an incline that formed along the NE-trending fractures (*Boutwell*, 1912). Economic minerals removed include galena, malachite, and tetrahedrite. The Ag, Pb, and Zn deposits are attributed to the Clayton Stock and were transported along the ENE trending Crescent Fault. The source of the smaller more recent Cu deposits is the altered Alta Stock (*John*, 1998). Gangue minerals include calcite, garnet, pyrite, and quartz (*Bromfield*, 1989).

The MicroDEM GIS software written by Peter Guth of the U.S. Naval Academy was used to compare the calculated orientation of the outcrops north of Scott's Pass with the measured data. The software is capable of a three-point analysis, which yields an outcrop trace and bedding orientation. This tool proved useful because outcrops in this region were highly jointed and provided few ideal surfaces for measurements (Figure 4). However, the Thaynes Formation outcrop was easily identified on the LIDAR image and it only took a few moments to find the bedding orientation. The calculated output was 295°, 35°, which closely correlated to the 300°, 30° measured in the field. Also, the northeast trending step faults were difficult to locate on foot but were visible on the LIDAR (Figure 3).

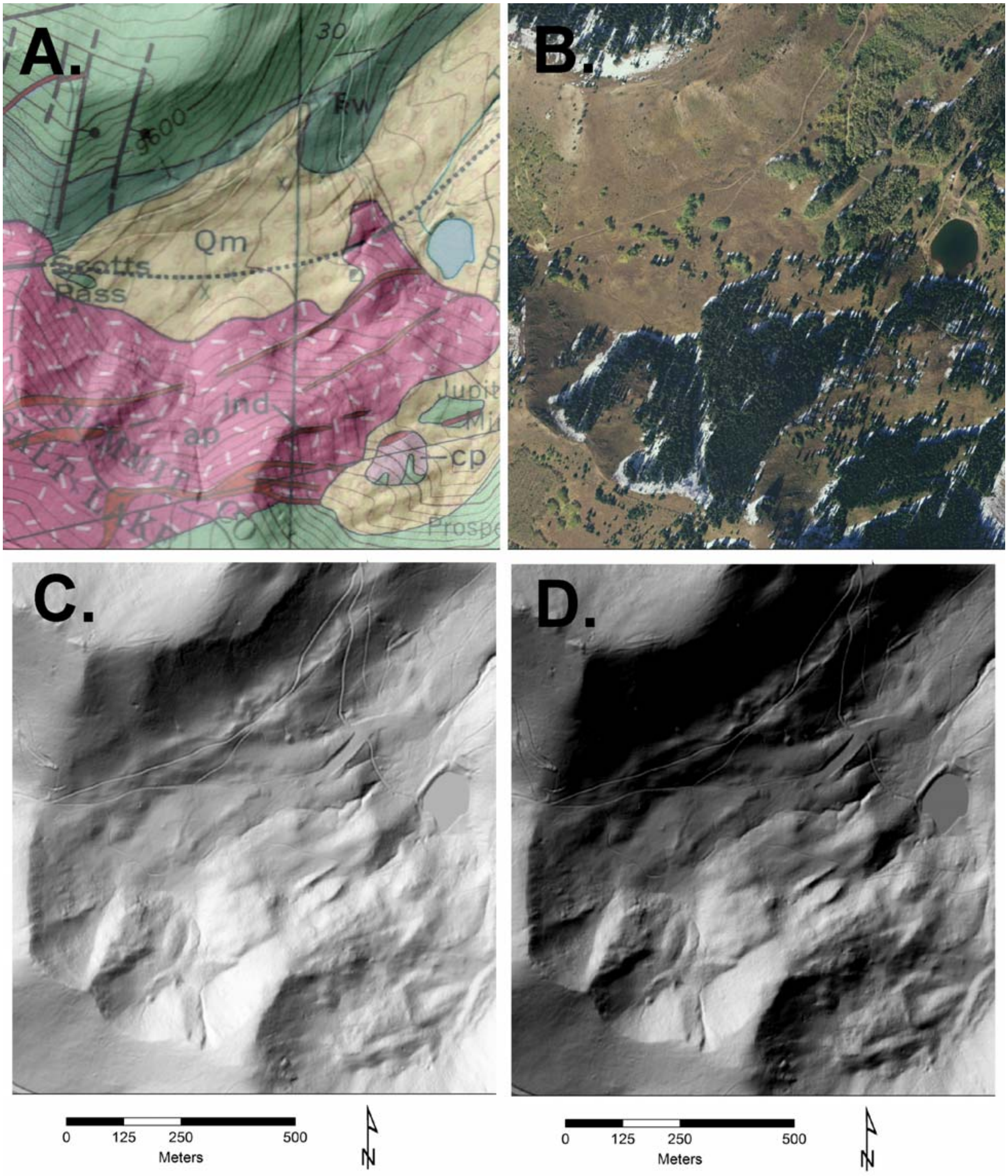

Figure 3. A. Geologic map of the Shadow Lake area, Alta mining district (from Baker et al., 1966). B. National Agricultural Imagery Program (NAIP) photograph of the area in A. C and D. Hillshades of LiDAR-derived DEMs from B.

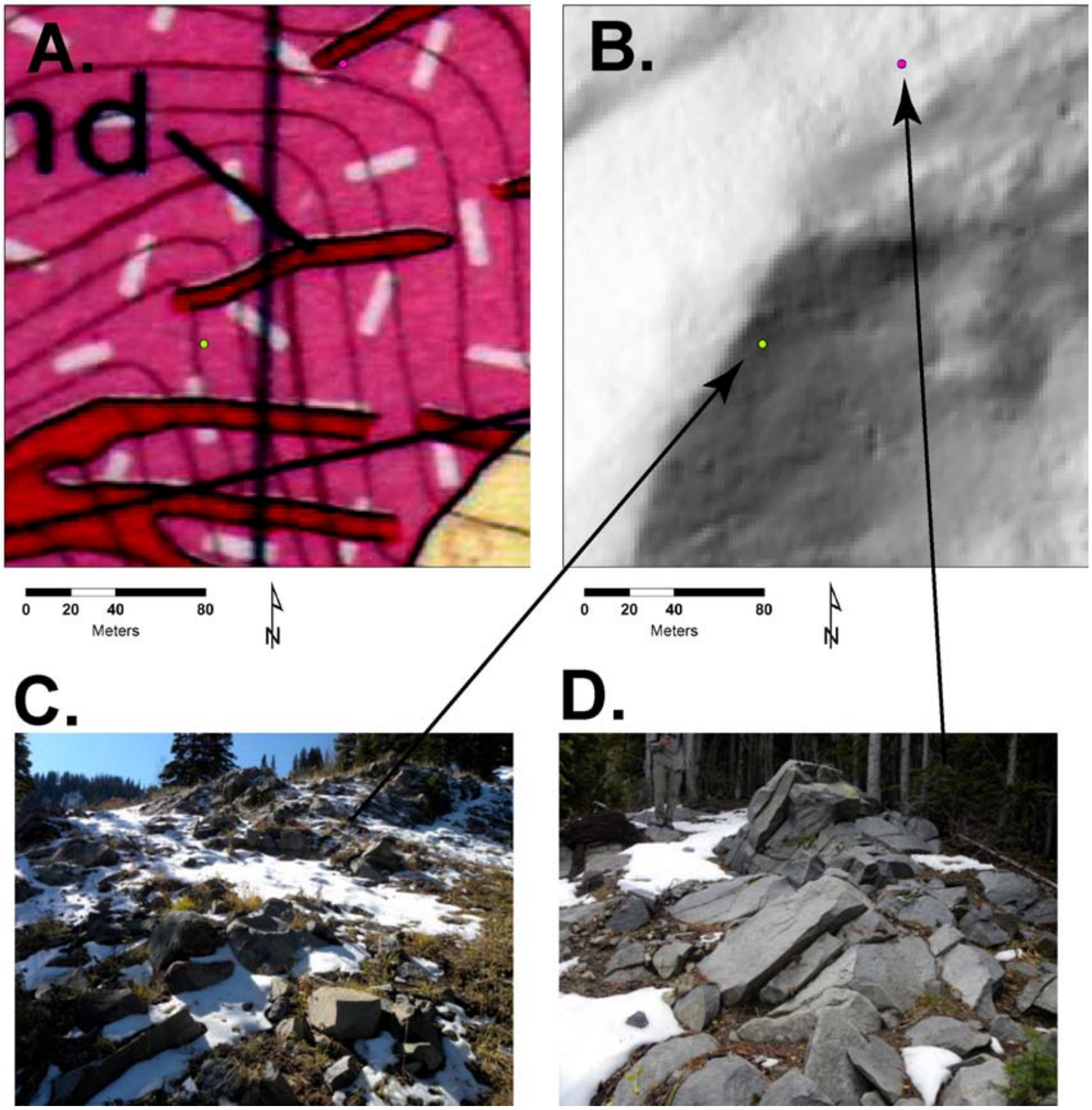

Figure 4. A. Detail of geologic map of the Shadow Lake area, Alta mining district (from Baker et al., 1966). Pink represents granodiorite of the Clayton Peak stock and dark red is intermediate dike material that has intruded the stock. B. Hillshade of LiDAR-derived DEMs. C. Field photo of Clayton Peak stock outcrop. D. Field photo of intermediate rock intruded into the Clayton Peak stock

<u>White Pine.</u> The White Pine area does not contain major historical mining but was examined in the fall, 2011 to see if LiDAR could highlight alteration features in the Little Cottonwood Stock in an area of dense vegetation. The geology is dominated by granite of the Little Cottonwood stock that is strongly pyritized over an extensive area (*Crittenden*, 1965). No mapped faults are visible in the area. The LiDAR coverage of the area shows little in the way of visible structure within the pluton, even within the highly pyritized Little Cottonwood granite (Figure 5).

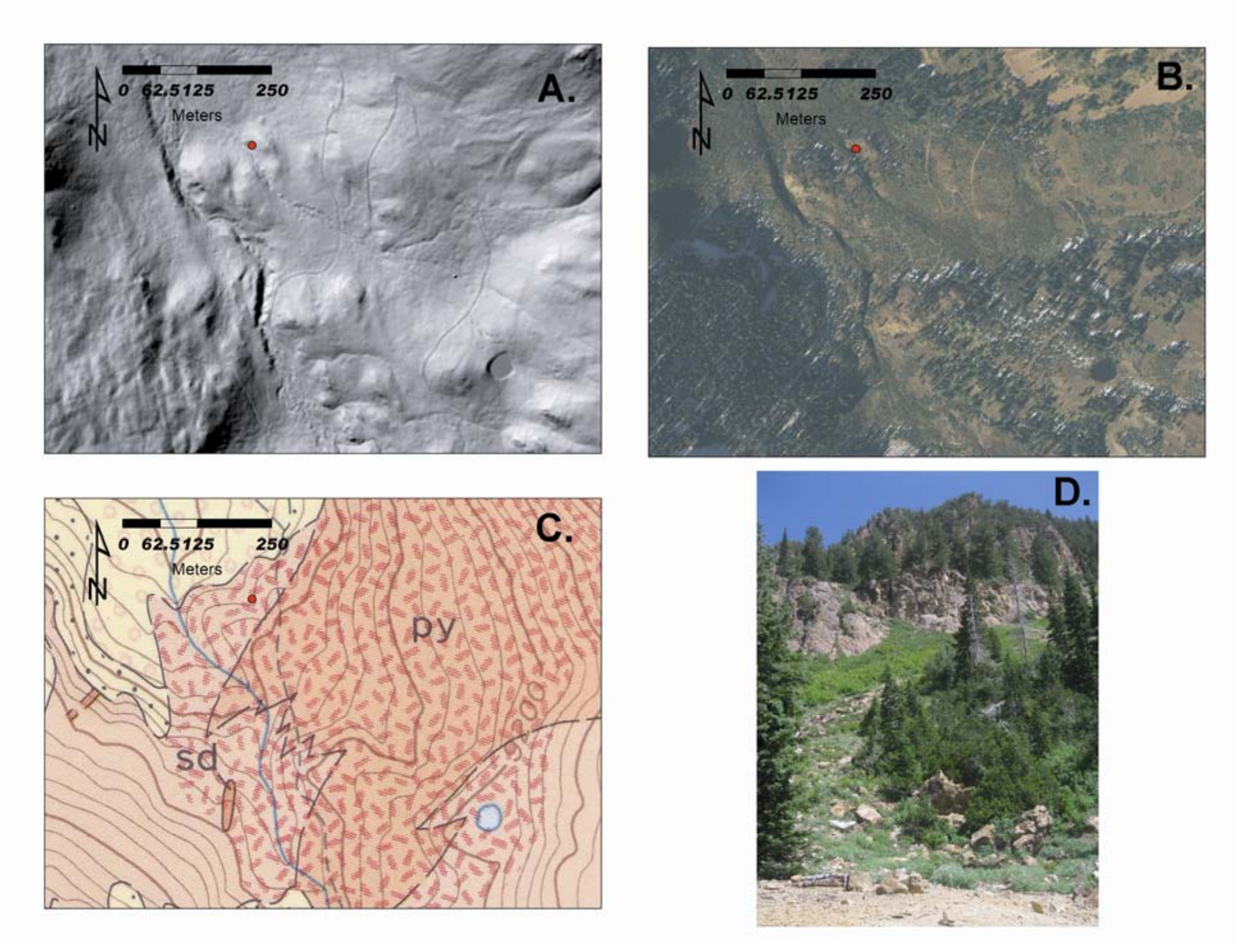

Figure 5. A. Hillshade of LiDAR-derived DEMs from the White Pine area, Alta mining district, Utah. B. National Agricultural Imagery Program (NAIP) photograph of the area in A. C. Geologic map of the Shadow Lake area, Alta mining district (from Baker et al., 1966). D. Field photograph of pyritized granite outcrop of the Little Cottonwood stock (courtesy of Ryan Hamilton).

Mill D. The Mill D area is located along a tributary of Big Cottonwood Creek, north of the drainage divide with Little Cottonwood Creek and has a number of historic mining areas in an area of structurally complex geology. Cambrian and Mississippian sliciclastics and carbonates are cut by thrust and normal faults of varying displacements (*Crittenden*, 1965). The most important ore deposit in the area is the Cardiff ore deposit which consists of base-metal sulfides largely found at the intersection of thrust faults (*Calkins and Butler*, 1943)

LiDAR imagery was only moderately successful in delineating geologic features of the area (Figure 6), such as normal faults between the sedimentary units. However, in the vicinity of dumps from the Cardiff mine workings, LiDAR illuminates material that is not visible with aerial photography (Figure 7).

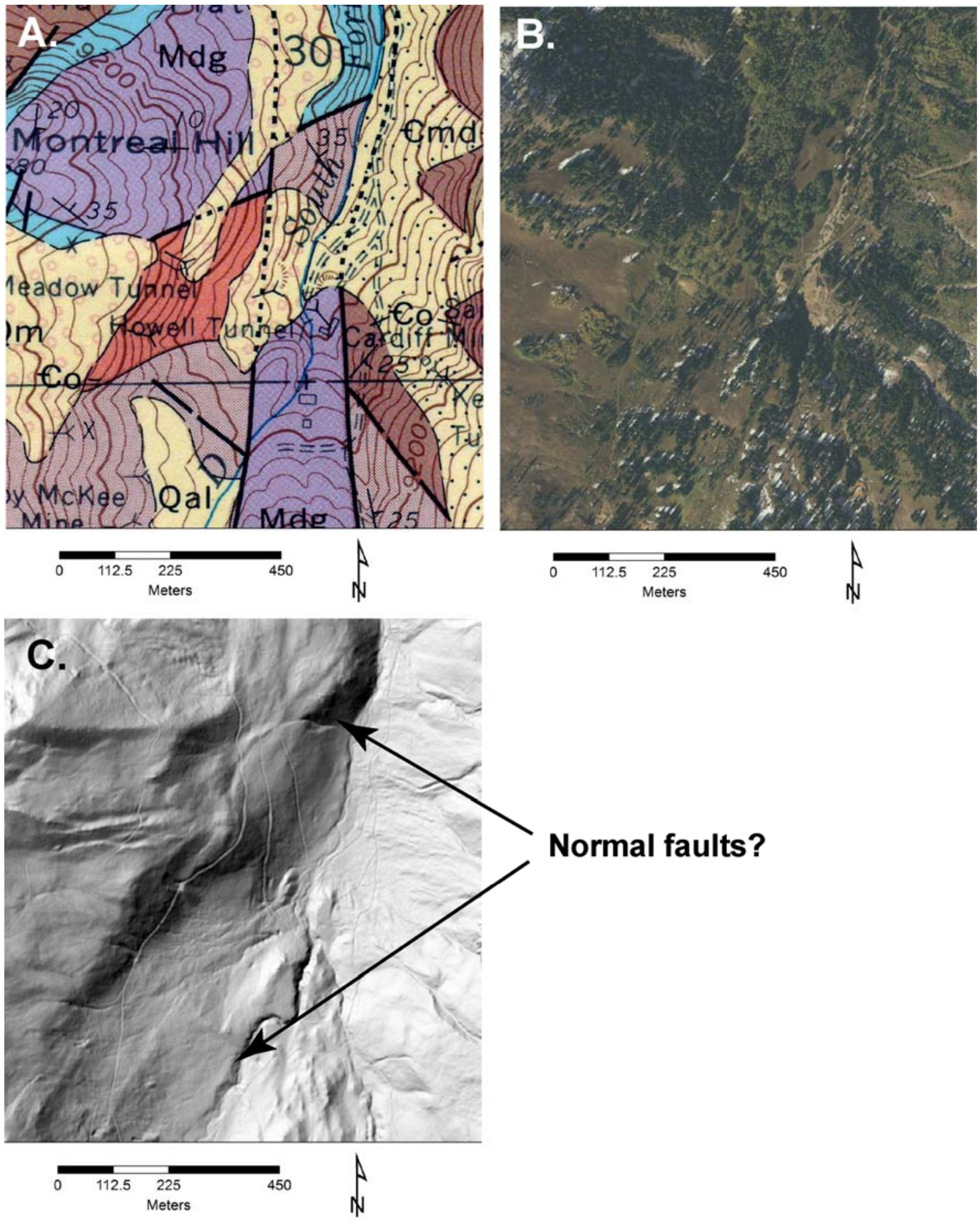

Figure 6. A. Geologic map of the Mill D area, Alta mining district (from Crittenden, 1965). B. National Agricultural Imagery Program (NAIP) photograph of the area in A. C. Hillshade of LiDAR-derived DEMs from the Mill D area, Alta mining district, Utah.

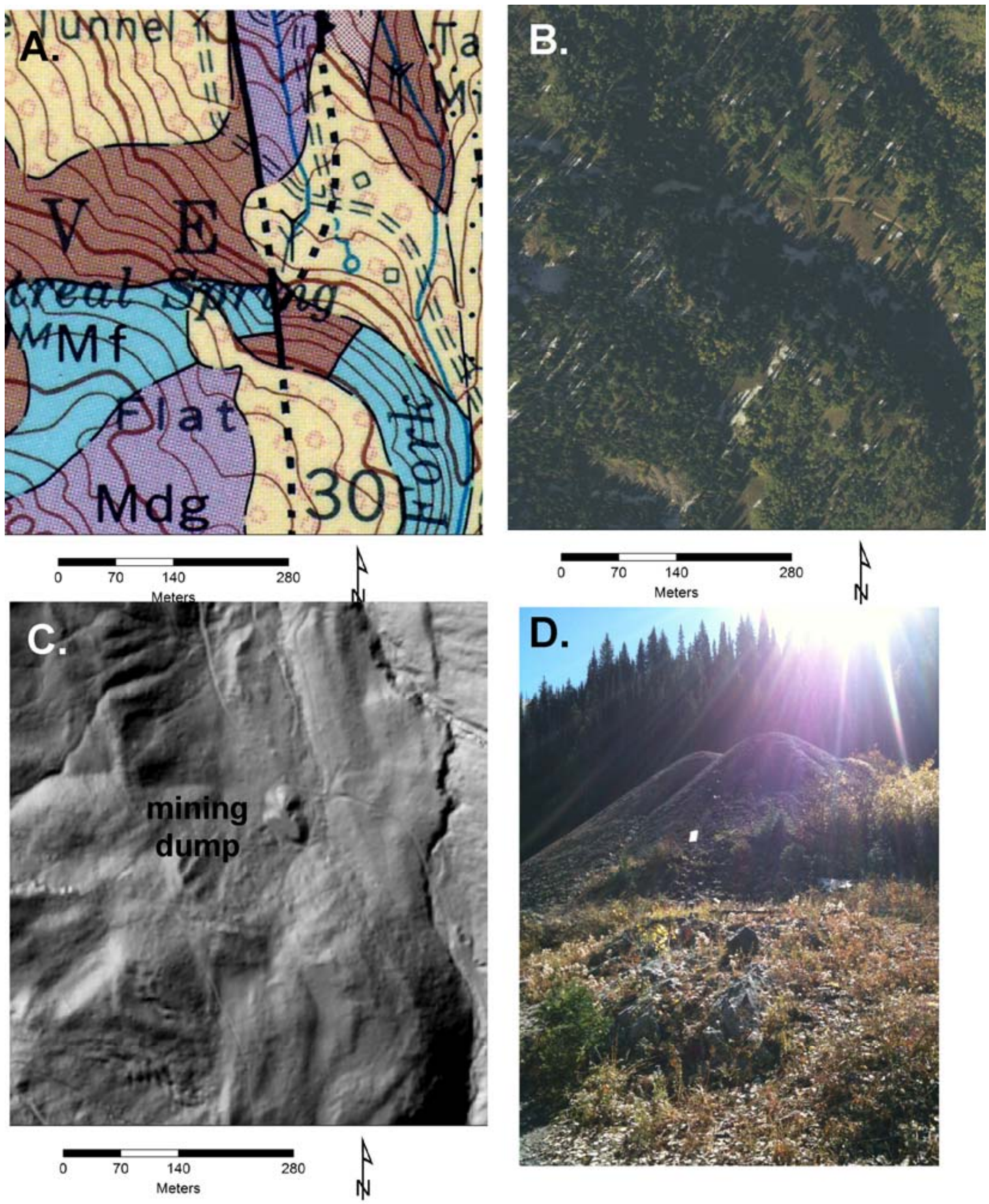

Figure 7. A. Geologic map of the Mill D area near the Cardiff mine, Alta mining district (from Crittenden, 1965). B. National Agricultural Imagery Program (NAIP) photograph of the area in A. C. Hillshade of LiDAR-derived DEMs from the Mill D area, Alta mining district, Utah. D. Field photograph of mine dump near the Cardiff mine (courtesy of Kimberlee Pulsipher).

Frisco District (Utah)

The Frisco mining district is located in the San Francisco Mountains ~40 km west of Milford, Utah (Figure 1). Although the Horn Silver Mine in the eastern portion of the district was a large producer of silver and base metals in the late 19th and early 20th centuries (*Butler*, 1913, 1914), very little modern geologic research has been conducted on the district. Rocks are largely lower Paleozoic carbonates intruded and extensively altered by granodiorite of the Oligocene Cactus stock and smaller, unnamed instrusive bodies (*Hintze et al.*, 1984). The majority of the mineralization consists of contact replacement and fissure deposits associated with the Cactus stock. Major ore deposits are found in both the instrusive rocks and as replacements of the surrounding carbonates with significant oxidation of the sulfides in the upper portions of the deposits (*Butler*, 1914).

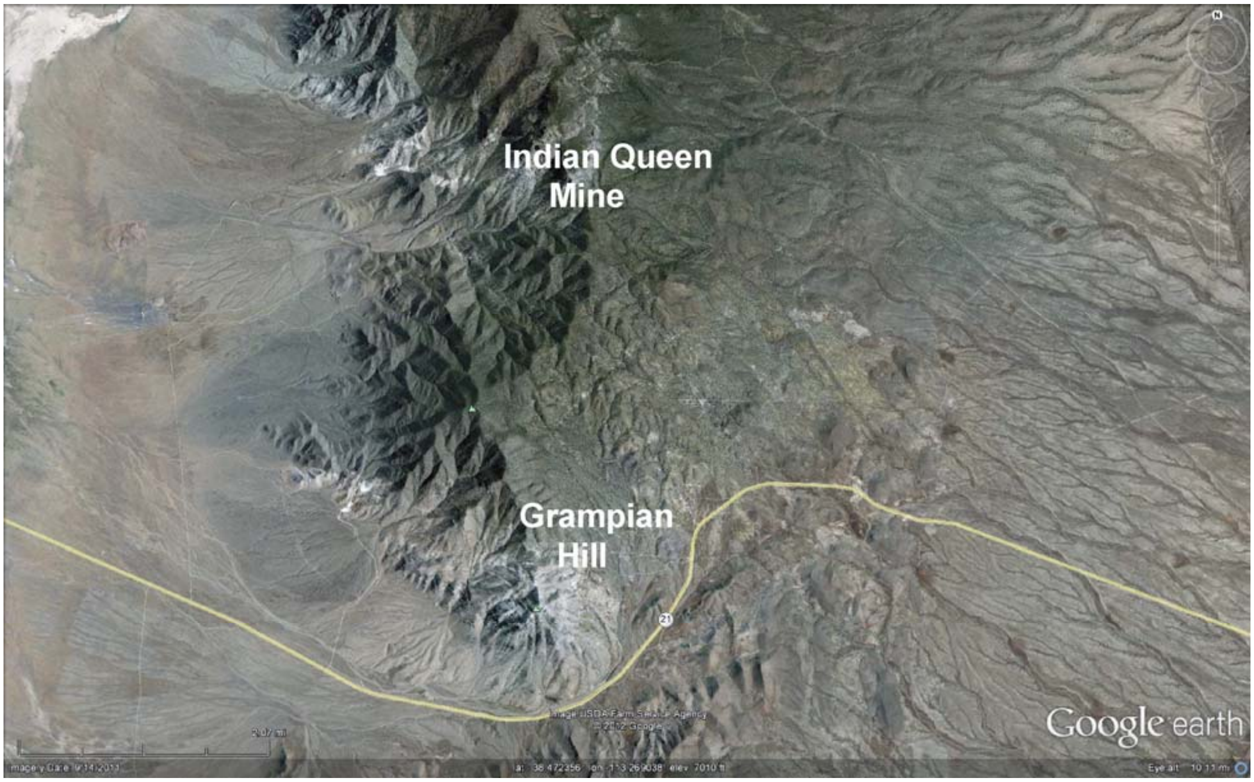

Figure 8. Location of the mineralized areas examined within the Frisco mining district, west-central Utah.

Indian Queen. The area north of the Indian Queen mine was examined in detail for two reasons (1) multiple alteration features in the metamorphic contact zone and (2) the ability to consider what alteration features are visible in LiDAR data that had obvious flaws. The area consists of a small (~10 ha) open pit area near a contact zone between the Cambrian Big Horse Limestone and the Oligocene Cactus stock. Details of the area, the quality of the LiDAR data, and various geologic features of the area are provided in Jewell et al. (*2013*).

Grampian Hill. The Grampian Hill area is located immediately north of State Highway 21 connecting the Milford and Wah Wah valleys. The area is characterized by limestones of uncertain age with extensive faulting and alteration. A small intermediate composition stock is present in the area, but appears not to be directly related to the extensive silicification of the limestone to the southwest. The LiDAR derived DEMs of the area clearly show the silicified limestones in the area, although they tend to be on the same strike and have the same topographic expression as unaltered limestone. The intrusive rocks in the area are visible on the photograph but have no particular topographic expression (Figure 9).

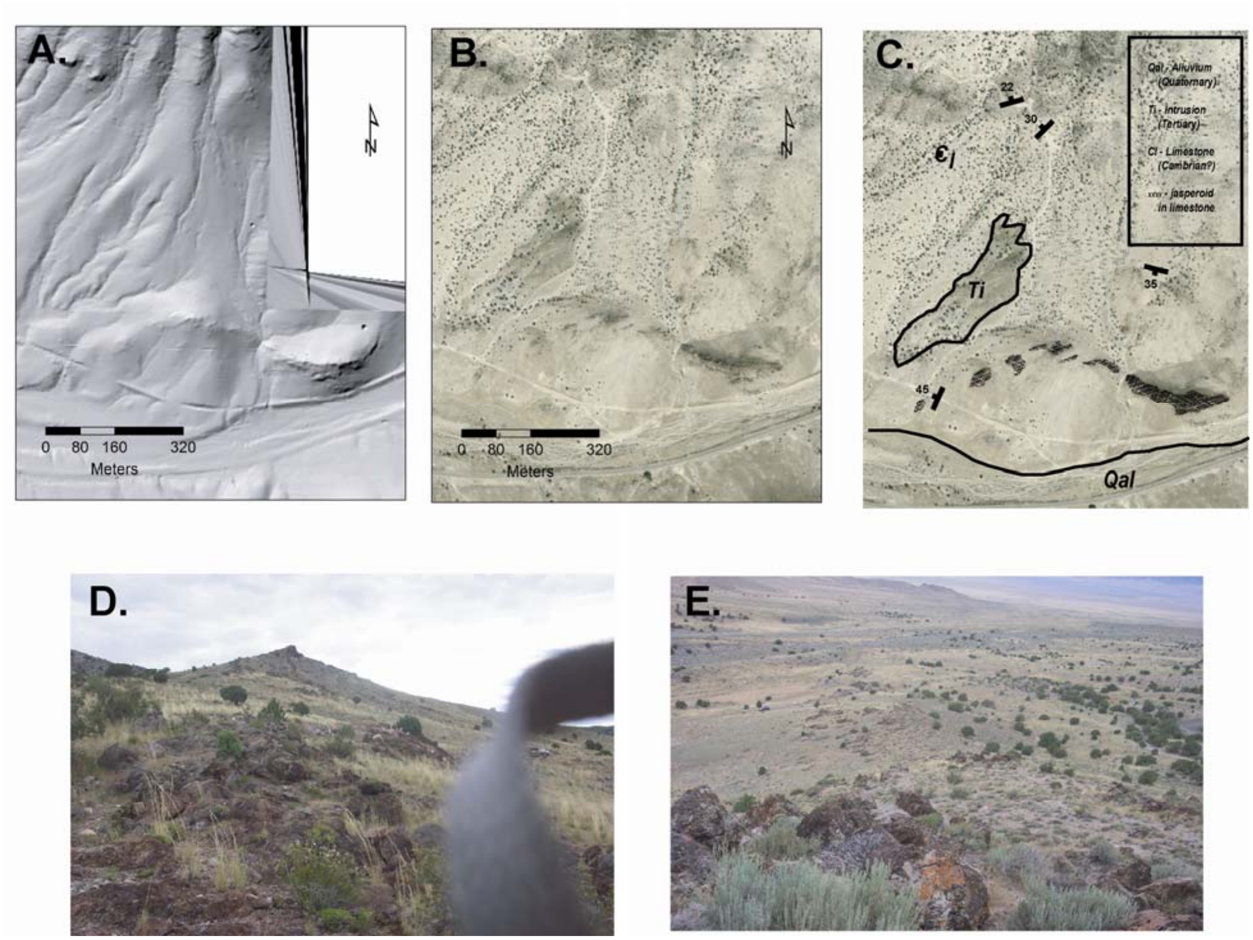

Figure 9. A. Hillshade of LiDAR-derived DEMs from the Grampian Hill area, Frisco mining district, Utah. B. National Agricultural Imagery Program (NAIP) photograph of the area in A. C. Simple geologic map of the area in B. D, E. Field photographs of silicified jasperoid in the Grampian Hill area

North Santiam District (Oregon) (contribution by Theresa Zajac)

The majority of the volcanic rock type found in 1,000 vertical feet of exposure along the Little North Santiam River is oligoclase andesite. Labradorite andesite is found in localized areas. The tops of ridges in the district are comprised of hypersthenes andesite. Most of the intrusive dikes in the district are comprised of dacite porphyry that typically trend to the northwest. The primary mineralization in the North Santiam District is chalcopyrite, sphalerite, pyrite, galena, and gold. The vein classifications are as follows:

1) Complex sulfide veins with sphalerite as the primary sulfide and variable amounts of pyrite, galena, and chalcopyrite

2) Pyrite veins with pyrite as the primary sulfide and variable amounts of chalcopyrite, sphalerite, and galena
3) Bimetallic veins which are a transition between complex sulfide veins and pyrite veins
4) Chalcopyrite veins with chalcopyrite as the primary sulfide and variable amounts of pyrite, sphalerite, and galena.

The primary gauge minerals in the district are quartz and calcite. The alteration within the district is sericitic and propylitic alteration with localized argillic alteration. Epidote, chlorite, sericite, calcite, quartz, and clay minerals around veins and on fractures are evidence of these alterations. Iron alteration is found within the district and is the result of weathering (*Callaghan and Buddington*, 1938). The two most important mines (Blue Jay and Ruth) and additional prospects are located near the headwaters of the Little North Santiam River. The features of the Blue Jay mine are discussed in detail in Jewell et al. (*2013*). The Ruth mine has many similar features: north-northwest trending fissures with base metal sulfides and minor gold. A number of small prospects immediately to the west of the Ruth and Blue Jay mines were examined, mostly along an access road to the upper portions of the Little North Santiam River.

South Santiam/Blue River District (Oregon) (contribution by Theresa Zajac)

Andesite with phenocrysts of oligoclase or andesine is the dominant volcanic rock found in the Blue River District. Labradorite andesite is also found in the district, but is not as abundant. The prophyritic augite diorite is the primary intrusive rock. The diorite intrusive bodies trend to the northwest. Near the contacts of intrusions, narrow aureoles of hornfels are found. The primary mineralization in the Blue River District is chalcopyrite, pyrite, sphalerite, and galena. The sulfides in the district contain very low amounts of precious metals. The main veins mined within the district are as follows:

1) Rowena vein with chalcopyrite as the primary sulfide and minor amounts of pyrite and sphalerite
2) Great Northern vein is primarily calcite with minor amounts of sulfides
3) Lucky Boy Mine vein with pyrite as the primary sulfide with variable amounts of galena, sphalerite, and chalcopyrite

There are other veins that contain varying amounts of sulfides, but majority are sphalerite rich. In weathered zones, small amounts of chrysocolla, malachite, cerusite, anglesite, and limonites are found. Weathered calcite veins contain brown manganese oxides. Quartz and calcite are the primary gauge minerals in the district (*Callaghan and Buddington*, 1938).

Few surface manifestations of old workings in the district are still visible on the ground and only one area was located on LiDAR DEMs (Figure 10).

Figure 10. A. Hillshade of LiDAR-derived DEMs from the Blue River mining district, Oregon. B. National Agricultural Imagery Program (NAIP) photograph of the area in A. C, D. Field photographs of minor prospect shown in the center of A. and B.

Grant County (Oregon)

A variety of historic mining operations are found in Grant and Baker Counties of northeastern Oregon (Figure 11). The geology of this area is dominated by a variety of Middle Devonian to Late Jurassic oceanic affinity rocks intruded by Late Jurassic-Early Cretaceous plutons (*Vallier and Brooks*, 1995; *Schwartz et al.*, 2011). The area north and south of the Middle Fork of the John Day River contains numerous historic vein gold deposits (*Allen*, 1951) and while linear features were clearly visible in the LiDAR-derived DEMs, none could be definitively related to observed mineralized structures on the ground (Figure 12).

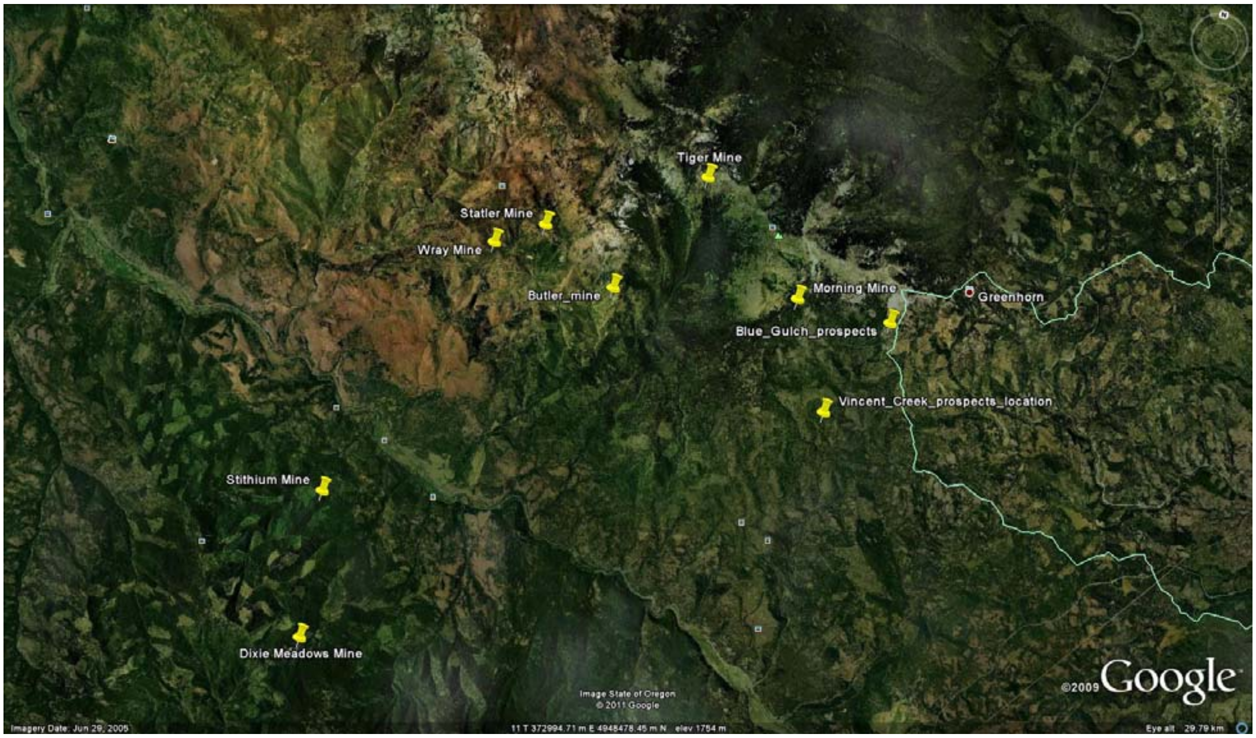

Figure 11. Location of the mineralized areas examined within the northeast portion of Grant County, west-central Utah.

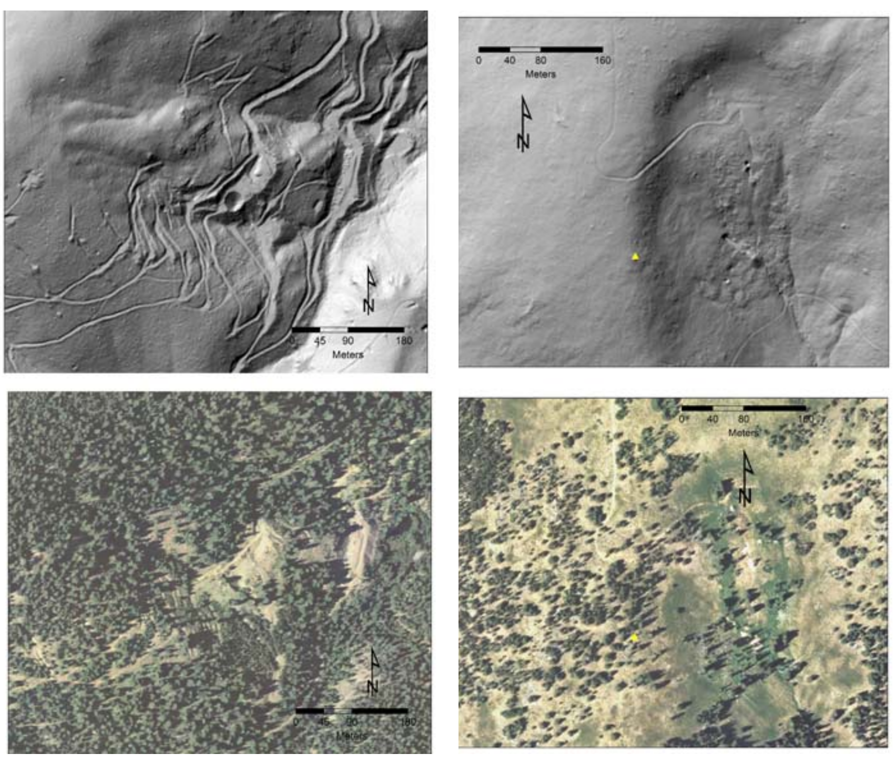

Figure 12. Examples of field area examined during 2011 field season. Dixie Meadows mined area and complex (left) and Tiger Mine area (right).

DISCUSSION

Until the mid-20th century, the United States economy benefitted from the confluence of favorable geologic provinces (principally in the Intermountain West); simple, straightforward federal mineral entry laws; and excellent training of earth scientists to locate and produce an abundance of non-fuel mineral commodities. The outlook for the 21st century is much less certain: most mineral deposits close to the surface in the arid Intermountain West have been found and mineral entry into much federal land, particularly in high elevation forested terrain, is now restricted by wilderness designation or study areas.

In order for the U.S. to maintain a strong position in mineral production, new deposits must be located (1) at greater depths in mature mining districts or (2) in areas that are prospective but have not received as much attention as the traditional mining provinces of the western U.S. Examples of this latter category include the Precambrian terrains of the upper Midwest (for instance the high-grade Eagle copper-nickel deposit brought into production recently by Rio Tinto in the Upper Peninsula of Michigan) and the majority of Alaska that remains open to mineral entry. Both of these areas are characterized by extensive boreal forest cover masking much of the geologic outcrops that can point the way toward potential ore deposits. Therein lies the promise of developing protocols for integrating airborne LiDAR into standard mineral exploration strategies.

It is envisioned that LiDAR could eventually become a complementary technique to more traditional airborne geophysical methods. A large expense of any airborne geophysical survey is operation of the airborne platform (be it fixed wing or helicopter). Thus the current expense of airborne LiDAR surveys (estimated to be \$200-\$500/km^2) could be pared down considerably were it mounted in the same aircraft as other geophysical instruments.

REFERENCES

Allen, R. M., Structural control of some gold-base metal veins in eastern Grant County, Oregon: Economic Geology, v. 46, p. 398-403.

Baker, A.A., Calkins, F.C., Crittenden, M.D., JR., and Bromfield, C.S., 1966, Geologic Map of The Brighton Quadrangle, Utah: *U.S.Geological.Survey Geologic Quadrangle Map GQ-534.*

Boutwell, J. M., 1905, Economic geology of the Bingham mining district, Utah. *U. S. Geological Survey Professional Paper 38* , 413 p.

Bromfield, C.S., 1989, Gold deposits in the Park City mining district, Utah, *U.S. Geological Survey Bulletin 1857-C*, pp. C14-C26.

Butler, B. S., 1913, Geology and ore deposits of the San Francisco and adjacent districts, Utah, *U. S. Geological Survey Professional Paper 80*, 212 p.

Butler, B. S., 1914, Geology and ore deposits of the San Francisco and adjacent districts, Utah, Economic Geology, v. 9, p. 412-434.

Calkins, F. C., and Butler, B. S., 1943, Geology and ore deposits of the Cottonwook-American Fork area, Utah. *U. S. Geological Survey Professional Paper 201*, 152 p.

Callaghan, E. and Buddington, A. F., 1938, Metalliferous mineral depsits of the Cascade Range, Oregon. *U. S. Geological Survey Bulletin 893*, 141 p.

Crittenden, M. D., Jr., 1965, Geology of the Dromedary quadrangle, Utah. *U.S. Geological Survey Geologic Quadrangle Map GQ-378.*

Harding, D. J., and G. S. Berghoff, 2000, Fault scarp detection beneath dense vegetative cover: airborne LiDAR mapping of the Seattle fault zone, Bainbridge Island, Washington state. *Proceedings of the American Society of Photogrammetry and Remote Sensing annual conference*, Washington, D.C.

Hedenquist, J. W., A. R. Aribas, and E. Gonzalez-Urien, 2000, Exploration for epithermal gold deposits, in Gold in 2000, S. G. Hageman and P. E. Brown, eds., *Reviews in Economic Geology*, v. 13, p. 245-277.

Jewell, P. W., Farnsworth, J. A., and Zajac, T., 2013, Rediscovering the discovery outcrop: the promises and pitfalls of LiDAR technology in mineral exploration: *Society of Exploration Geologists Newsletter,* v. 92, p. 1, 12-16.

John, D.A., 1998, Geologic setting and characteristics of mineral deposits in the central Wasatch Mountains, Utah, Geology and ore deposits of the Oquirrh and central Wasatch Mountains, Utah: *Society of Economic Geologists Field Guidebook Series no. 29,* p. 11-33.

LaMaskin, Vervoort, J. D., Dorsey, R. J., Wright, J. E., 2011, Early Mesozoic paleogeography and tectonic evolution of the western United States: Insights from detrital zircon U-Pb geochronology, Blue Mountains province, northeastern Oregon: *Geological Society of America Bulletin, v. 123,* p. 1939-1965.

Lovering, T. S., 1972, Jasperoid in the United States – Its characteristics, origin, and economic significance: *U. S. Geological Survey Professional Paper 710,* 164 p.

Schulz, W. H., 2005, Landslide susceptibility estimated from mapping using light detection and ranging (LiDAR) imagery and historical landslide records, Seattle Washington. *U. S. Geological Survey Open File Report 2005-1405*, 13 p.

Vallier, T. L., and Brooks, H. C., 1995, Geology of the Blue Mountains region of Oregon, Idaho, and Washington: Petrology and tectonic evolution of pre-Tertiary rocks of the Blue Mountains region: *U.S. Geological Survey Professional Paper 1438*, 540 p.

Appendix A. Summary of field localities investigated.

Location	**Host rock**	**Alteration type**	**Commodity**	**Surface manifestation**	**Application of LiDAR**
Oregon					
North Santiam Ruth Blue Jay Misc.along Little North Santiam River	Oligocene volcanics	Minor silicification	Gold, base metals	Linear features corresponding to vein orientation?	Identification of stream linears corresponding to vein orientation; outcrop, historic workings in heavy vegetation
Blue River	Oligocene volcanics	Minor silicifiation, argillization	Base metals	None noted	Unsuccessful
Camp Creek Stithium Dixie Meadows Tiger Statler	Mesozoic volcanics, metabasalts	Pervasive serpentin-ization	Gold, base metals	None noted	Numerous visible faults; no correlation with mineralized structures
Utah					
Alta White Pine Shadow Lake Mill D	 Oligocene intrustive Triassic siliciclastics, carbonates Middle Paleozoic carbonates	 Vein Skarn, fissures Skarn, fissures	Silver, base metals	 None noted Extensive faulting Subtle expression of faulting	 Unsuccessful Numerous visible faults Possible manifestations of faulting
Frisco Indian Queen Grampian Hill	 Cambrian Limestone Cambrian Limestone	 Skarn Silicification along faults	Silver, base metals	 Silicification of faults	 Identification of prominent silicification